

PAPER • OPEN ACCESS

## A New Concept of Direct Oil Cooling System for AFPM Machines, Numerical Analysis and Optimization

To cite this article: L. Pirillo *et al* 2024 *J. Phys.: Conf. Ser.* **2685** 012020

View the [article online](#) for updates and enhancements.

You may also like

- [Economic Evaluation of Seawater Cooling System Applying Flooded Type Evaporator](#)  
Jung-In Yoon, Chang-Hyo Son, Choon-Geun Moon *et al.*
- [A scalable helium gas cooling system for trapped-ion applications](#)  
F R Lebrun-Gallagher, N I Johnson, M Akhtar *et al.*
- [Car Cabin Cooling System Using Solar Energy](#)  
Rifky and Oktarina Heriyani

**PRIME**  
PACIFIC RIM MEETING  
ON ELECTROCHEMICAL  
AND SOLID STATE SCIENCE

HONOLULU, HI  
Oct 6–11, 2024

Abstract submission deadline:  
**April 12, 2024**

Learn more and submit!

**Joint Meeting of**  
The Electrochemical Society  
•  
The Electrochemical Society of Japan  
•  
Korea Electrochemical Society

# A New Concept of Direct Oil Cooling System for AFPM Machines, Numerical Analysis and Optimization

L. Pirillo<sup>1</sup>, F. Nardecchia<sup>2</sup> and F. Bisegna<sup>3</sup>

<sup>1</sup> Ph.D. Student, Department of Mechanical and Aerospace Engineering, Via Eudossiana 18, Roma (RM), 00184, Italy.

<sup>2</sup> Ph.D., Department of Astronautic, Electric and Energy Engineering, Via Eudossiana 18, Rome (RM), 00184, Italy.

<sup>3</sup> Associate Professor, Department of Astronautic, Electric and Energy Engineering, Via Eudossiana 18, Rome (RM), 00184, Italy.

lorenzo.pirillo@uniroma1.it

**Abstract.** Given the strong growth of the electric drive industry, the automotive sector needs to increase the power density of its motors, leading to a size decrease and, consequently, to economic savings. The increase in power density brings with itself the consequence of increasing the Joule effect losses in the active conductors of the machine. For this reason, the problem of cooling turns out to be of utmost importance precisely because of its direct coupling with mechanical and electromagnetic design. This paper has the aim to perform a CFD analysis concerning the cooling system of a permanent magnet axial flux electric machine. The innovative cooling system studied is a direct one which takes advantage of oil to cool down the DC powered coils. The innovation brought by the present research lays in both the direct axial ejection and the use of oil as coolant. At the current state of art, the coolant flows tangentially and, moreover, water is usually employed instead of oil. The main aim of this analysis will be, after a validation of the numerical code by comparison of the literature data, to minimize the maximum temperature of the coil by means of the proper positioning of the nozzle.

## 1. Introduction

The state of the art in AFPM machines has been rapidly advancing in recent years, due to the growing demand for high-efficiency electric motors. Overall, the state of the art in AFPM machines is characterized by a continuous push for higher power density, improved efficiency, and lower cost [1]. As the demand for electric motors continues to grow, it is likely that we will see further advancements in AFPM technology in the coming years [2]. The air gap flux permanent magnet (AFPM) machine is a promising technology that has gained significant attention in recent years due to its high torque density, compact size, and improved efficiency [3]. As the demand for higher power density and continuous operation under extreme conditions continues to rise, efficient cooling systems are crucial for managing the generated heat and ensuring optimal performance of AFPM machines. Nowadays, the methods adopted for heat removal are several. There are traditional cooling methods, such as natural convection or surface cooling techniques [4][5] and forced convection cooling methods, involving the use of external fans or blowers to enhance the airflow and heat transfer within the machine [6][7]. Moreover, liquid cooling methods, including direct liquid cooling (DLC) and indirect liquid cooling (ILC), have shown significant potential in efficiently managing the heat generated by



AFPM machines. The choice of coolant and optimization of the cooling channel design are critical factors in achieving effective liquid cooling in AFPM machines [8][9]. Hybrid cooling configurations may involve a combination of air and different liquid cooling strategies. The design and optimization of these complex systems require comprehensive analyses and multi-physics simulations to ensure effective heat transfer and thermal stability [10].

The aim of this work is to analyse and optimize, using a CFD code, a new direct oil cooling system, [11][12] which consists in a direct axial ejection of the coolant. The final purpose is to optimize the nozzle position and size in order to maximize heat removal and consequently, minimize the maximum coil temperature.

## 2. Physical problem and methodology

Of the many models of electric machines for wheeled transport that exist in the current state of the art, Axial Flux Permanent Magnet (AFPM) machines are particularly promising because they offer a smaller axial footprint for the same power density with respect to their radial counterpart [13]. Nowadays, the most used cooling system used for these machines consists in enclosing the stator copper strip coils in a metal jacket [14], which is then cooled down by water flowing in annular channels (see Figure 1).

For the CFD simulations of the new concept cooling system, a 3-D CAD of the coil has been built and then partially enclosed in a fluid domain. In this way, the coolant can be injected in order to lap the upper surface of the coil, giving thus rise to a heat removal. The critical part of the coil, in terms of hotspot temperature, is the bottom one, which is the farthest from the heat sink.

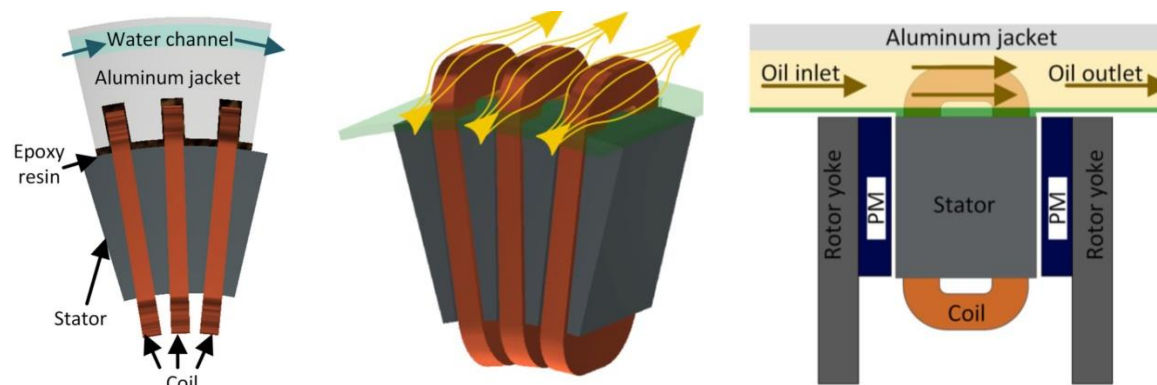


**Figure 1:** State of the art cooling system for AFPM Machines (left). New concept cooling system (centre and right).

## 3. Computational Setup

### 3.1. Test case description

The machine considered in this work has a stator pack and two rotor packs, coaxial to each other and arranged so that the stator, is placed between the two rotors and it is separated from them by two air gaps (left side of figure 2). The coils are located in the perimetral area of the stator core, and they are supplied with direct current (DC). The permanent magnets are housed on both rotors. The machine consists of 8 pole pairs, 48 stator slots in which each coil is housed, and it has as many nozzles responsible for the coolant ejection. The coolant is ejected axially, and it invests the coil as it is a fin [15]. It then descends by gravity into the area between the rotor and the coil and is then conveyed, together with all flows from the other nozzles, into a lower plenum. Then, a recirculating pump draws the fluid from the plenum and redistributes it as evenly as possible all over the machine's nozzles, thus

closing the cycle. The coil housed on the stator consists of a 'ribbon' conductor of section 1mm x 5mm of enamel-insulated copper. It consists of eight windings in order to create a rectangular structure with smoothed corners. In the context of this work, each winding of the coil has been 3-D modelled and then enclosed in a fluid domain. After that, a cylindrical nozzle has been obtained (right side of figure 2).

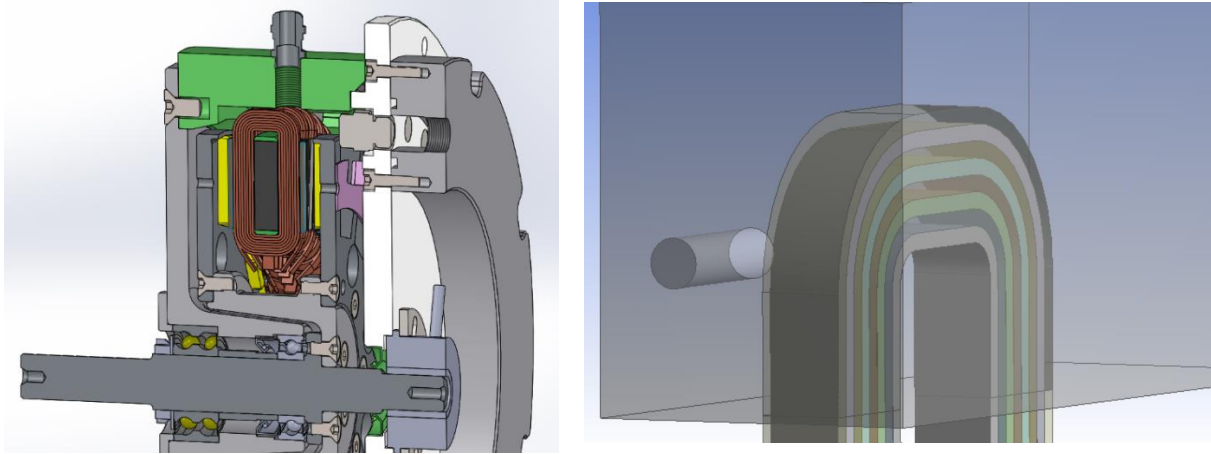


**Figure 2:** Detail of the machine (left). 3-D CAD of the eight strips of the coil, the fluid enclosure, and the nozzle (right).

### 3.2. Materials

The materials considered for this work are copper and enamel for the coil active material and insulator [15], while for the coolant a mineral transformer oil has been chosen. The physical parameters important for the analysis are reported in table 1.

**Table 1:** Thermophysical properties of the materials used in this work.

	Copper	Enamel	Oil
$\rho$ [kg/m <sup>3</sup> ]	8978	2719	780
$c_p$ [J/kg K]	381	871	3002
$\lambda$ [W/m K]	386	0.93	0.24
$\mu$ [Pa s]	-	-	0.0195

### 3.3. Parametrization test Matrix.

In this paper, a campaign of simulations has been performed, with the purpose of finding an optimal configuration for both the nozzle diameter (D) and its position (L), evaluated from the bottom of the fluid enclosed domain. Starting from the baseline configuration (Sim 5) which reproduces the experimental setup of [15] both D and L have been changed in order to obtain a matrix of 9 test cases, summarized in Table 2. Each case it runs with the same mass flow rate and inlet temperature in order to find the configuration which leads to a minimum hot spot temperature of the coil.

**Table 2:** Test matrix of simulations.

<b>D – L</b>	<b>3mm</b>	<b>5mm</b>	<b>7mm</b>
<b>10mm</b>	Sim 1	Sim 2	Sim 3
<b>12mm</b>	Sim 4	Sim 5	Sim 6
<b>14mm</b>	Sim 7	Sim 8	Sim 9

### 3.4. Numerical and Meshing Strategy

Given the axial symmetry of the machine, the analysis on which this work is based will be concentrated on an angular section equal to  $1/48$  of the revolution angle, i.e., on a single coil, to reduce the computational cost of the simulations, but still obtaining results representative of the behaviour of the entire machine.

The CFD simulation have been conducted with a pressure based coupled algorithm, they are steady state, one phase and viscous. The turbulence model adopted is the realizable k- $\epsilon$  with standard wall functions. A block-structured mesh [17] is chosen for the coil, in such a way that the layer of insulator between one winding and the next, which represents a lumped contact resistance is exactly halfway between two adjacent cells, which, by communicating, will take it into account in an optimal manner. In the fluid domain, the grid generated, consists of a tetrahedral structure in the bulk of the fluid and it contains a structured liner in the “near wall region”. The structured liner consists of 30 prismatic layers, whose height grows following a geometric sequence with growth rate equal to 1.2, starting from a first cell height of  $2.4 \mu\text{m}$ . in the downstream region of the fluid, the mesh size is increased in order to prevent pressure disturbances to rise back to the coil. A detail of the mesh is reported in figure 3.

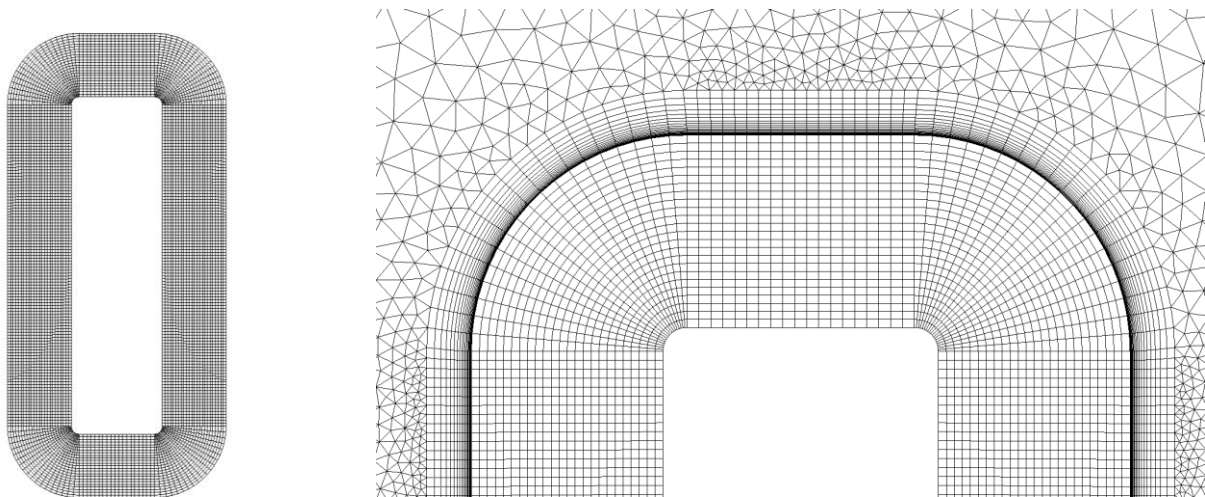


**Figure 3:** Mesh of the coil and the fluid, together with a detail of the near wall region refinement.

### 3.5. Initial and Boundary Conditions

The boundary conditions used for all the test cases investigated are the following:

- Mass flow inlet for the inlet section of the nozzle;
- Pressure outlet for the outlet plane;
- Wall with free slip for the fluid boundaries;
- Wall with no slip condition for the fluid-facing coil surfaces;
- Wall with thin layer and shell conduction for the coil-coil interfaces.

For each one of the cases under analysis it was assumed a thermal power generation inside the coil of 100 W [19]. The fluid field has been initialized by using constant parameters taken from the inflow.

## 4. Results

### 4.1. Validation

Both the numerical code and the mesh have been validated. A “mesh sensitivity analysis” was performed to obtain a convergent grid.

Four grids with a different degree of refinement have been built. They have been run with the same boundary conditions, and the results have been compared to each other. The features of the four grids are highlighted in table 3. The results, in terms of static temperature, have been extracted along the red line of figure 4, and they are reported together. Mesh 3 can be considered convergent, since the maximum difference between its results and Mesh 4 results is 1.92%, a value well below the limit for which mesh convergence can be declared.

After that, the software and the numerical method have been validated by comparison of the results with experimental data coming from literature. The experimental facility of [15] was reproduced in the simulation 5, in which the diameter of the nozzle is 5 mm and the distance of its centre, calculated from the bottom of the fluid domain (L) is 12 mm. the experimental data are well reproduced when the inlet velocity is 0.5 m/s and the inlet temperature is 25 °C, resulting in a hotspot temperature of the coil of 178°C.

**Table 3:** Features of the four different meshes created.

Mesh number	Number of cells	Average cell dimension [ $\mu\text{m}$ ]	First cell height [ $\mu\text{m}$ ]	Growth rate
1	650.000	500	2.4	1.2
2	980.000	97	2.4	1.2
3	1.270.000	35	2.4	1.2
4	1.550.000	1.1	2.4	1.2

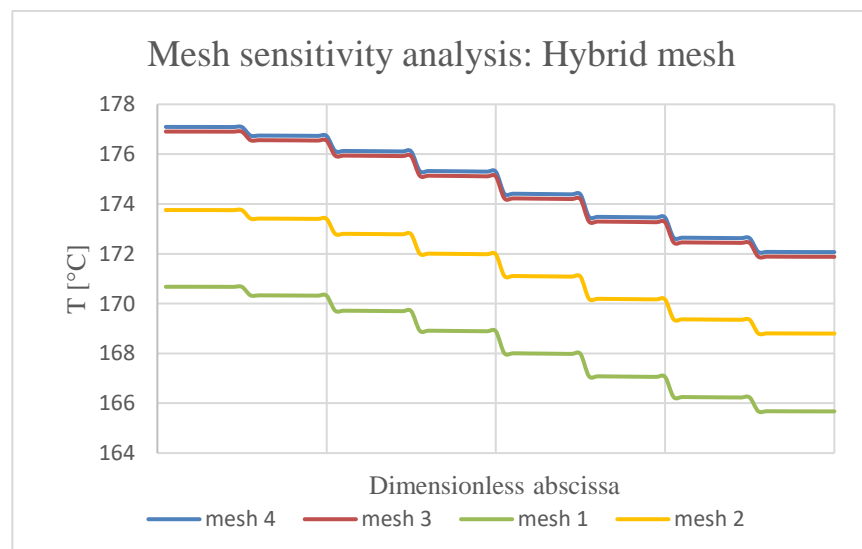
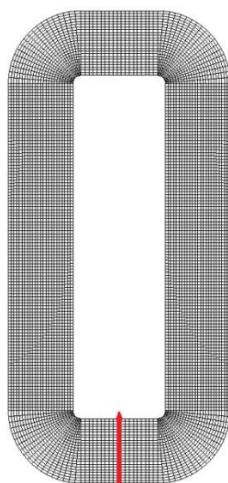


**Figure 4:** Temperature profile along the hot spot line for every mesh generated.

#### 4.2. Optimal Configuration

After the validation is performed, the test matrix of simulations presented previously is implemented to find the situation in which the hotspot temperature of the coil is minimum. All the cases have been carried out by keeping the value of the mass flow rate as a constant, which results in an increase of the inlet velocity in simulations 1, 4 and 7, and a decrease of it in simulations 3, 6 and 9, due to the change in the value of the nozzle diameter. An inlet temperature of 25 °C has been assumed for every simulation. The results have been extracted, for each one of the 9 simulations, along the hotspot line and they are presented aside in figure 5.

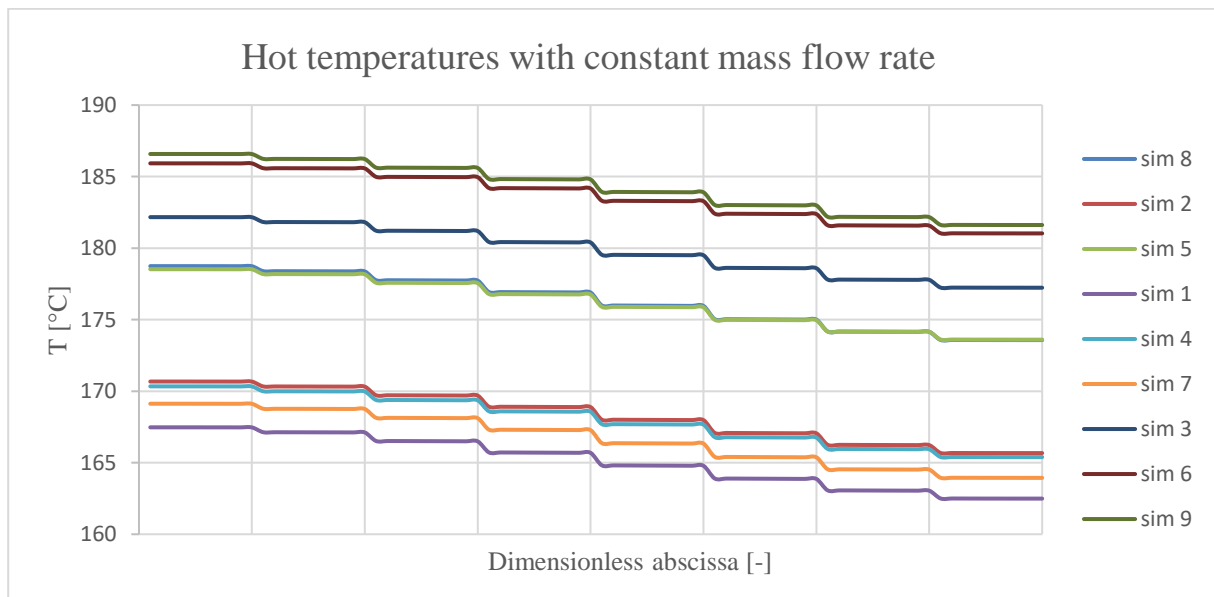


**Figure 5:** Hot temperatures of the coil for all the 9 simulations performed.

The simulation for which the minimum hot spot temperature of the coil is obtained is simulation 1, i.e. the one where the diameter is minimum and the nozzle height is maximum.

It can be seen that with the same diameter, for all 3 solutions, the best configuration is the one in which the nozzle is placed as high as possible. The nozzle placed at the top, although geometrically further away from the hot spot, is the one that results in the most effective cooling, no matter its diameter value, with an advantage that is more marked for intermediate diameters. The nozzle placed at the top is placed in a better position regarding the fluid motion established in the coil-fluid interface. In fact, given the curvature that characterizes the coil itself, injecting the fluid further down means that it interacts with the surface through a very large angle of attack (tending to 90°). In that case, the coil basically acts like a 'wall', and strongly slows down the fluid, severely penalizing the Reynolds number and the heat transfer. Injecting the fluid at the top, on the other hand, means adopting smaller angles of attack between the undisturbed flow and the coil surface. In this way, the reduction in velocity due to interaction with the coil is less pronounced, and the fluid is also able to effectively lap the coil in the downstream area, improving the amount of heat transferred. The three-dimensional streamlines are shown in figure 6 as a comparison between simulations 1 and 5.

For the purpose of heat removal, the most important comparison to be made is the value of the global heat transfer coefficient. Its behaviour is extracted along the midline of the coil's upper surface for all 9 simulations carried out and it is reported in figure 7. Simulation 1, which is the one that led to a lower value of the hot spot temperature, is the one with the highest values of the heat transfer coefficient. From these simulations, therefore, the solution to be adopted is to minimize the diameter of the nozzle and, secondly, to place it as high as possible according to geometric constraints.

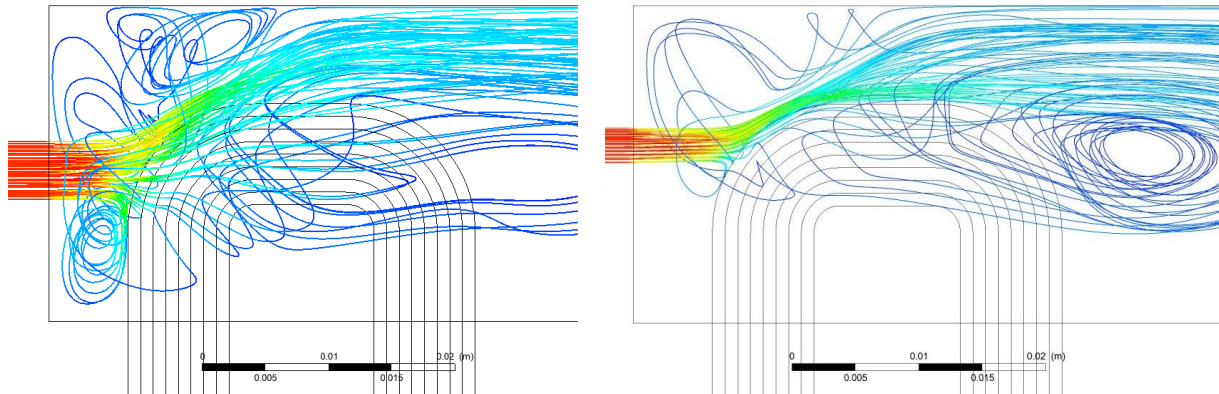


**Figure 6:** velocity streamlines coloured with velocity magnitude. Sim. 5 (left). Sim. 1 (right).

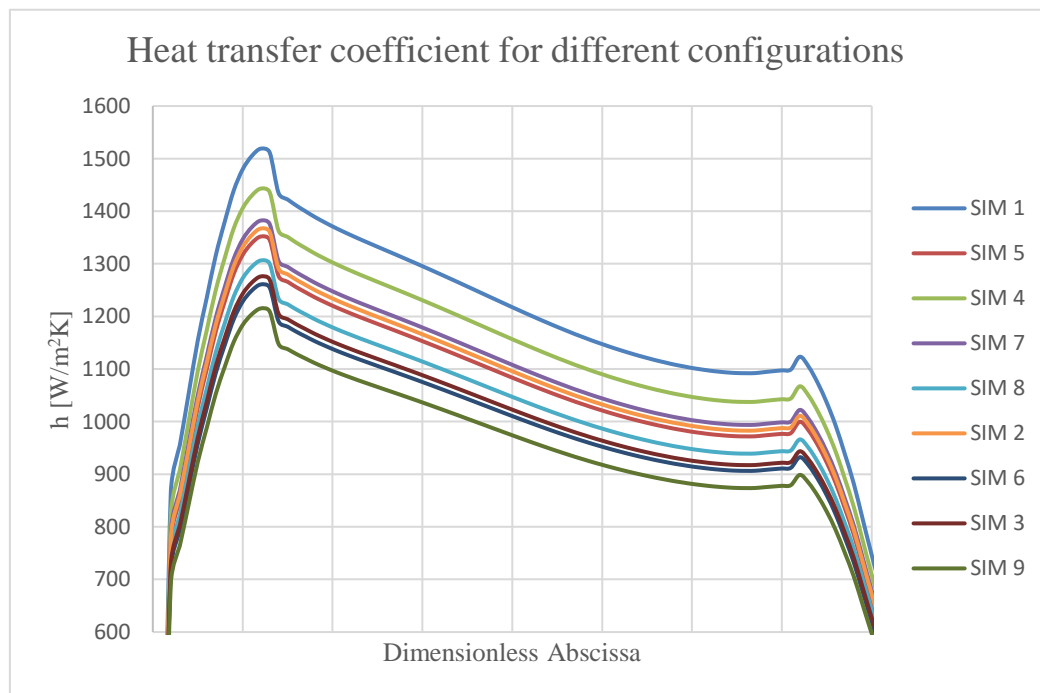


**Figure 7:** Heat transfer coefficient for each one of the simulations of the test matrix.

## 5. Conclusions

The analysis carried out during this paper highlighted the important improvements that a direct oil cooling system would bring to the state of the art. Moreover, by means of a CFD campaign, it was shown that the nozzle, responsible of the coolant injection, results in a more effective cooling of the coil when it is placed as high as possible (coherently with geometrical limits) and it is characterized by a small diameter, for the same mass flow rate. The reason for that is given by the strong decrease of velocity suffered from the impinging flow if the nozzle is located too low. Moreover, this work can be considered as a basis for further analysis and optimizations of AFPM cooling systems, and it can be extended also in other configurations in which the coils are not fixed in space or the fluid investing them is considered by means of a two species approach, together with the air permeating the domain.



## 6. References

- [1] Bhagubai P P C, Bucho L F D, Fernandes J F P and Costa Branco P J 2022 *Optimal Design of an Interior Permanent Magnet Synchronous Motor with Cobalt Iron Core. Energies* **15**(8) 2882
- [2] Hüner E and Toylan H 2022 *Design optimization with genetic algorithm of open slotted axial flux permanent magnet generator for wind turbines. Int. J. of Green Energy* **20**(4) pp 1-9
- [3] Kelch F, Yang Y, Bilgin B and Emadi A 2018 *Investigation and design of an axial flux permanent magnet machine for a commercial midsize aircraft electric taxiing system. IET Electrical Systems in Transportation* **8**(1) pp 52-60
- [4] Wan Z, Sun B, Wang X, Wen W and Tang Y 2020 *Improvement on the heat dissipation of permanent magnet synchronous motor using heat pipe. Proceedings of the Institution of Mechanical Engineers, Part D: Journal of Automobile Engineering* **234**(5) pp 1249-1259
- [5] Tikadar A, Johnston D, Kumar N, Joshi Y and Kumar S 2021 *Comparison of electro-thermal performance of advanced cooling techniques for electric vehicle motors. App. Th. Eng.* **183** (2) 116182
- [6] Liu Y and Lei G 2018 *Thermal analysis of an air-cooled air gap flux permanent magnet machine for hybrid electric vehicle. Energies* **11**(4) 880
- [7] Yao Z and Li S 2020 *Analysis and optimization of forced air cooling for air-gap flux permanent magnet machines. IEEE Transactions on Magnetics* **56**(1) pp 1-10
- [8] Mao W and Yang G 2021 *A comprehensive review of cooling techniques for air-gap flux permanent magnet machines. Energies* **14**(5) 1277
- [9] Deng W and Huang J 2020 *Thermal analysis and optimization of a direct liquid cooling system for an air-gap flux permanent magnet machine. IEEE Transactions on Magnetics* **56**(3) pp 1-10
- [10] Chen X and Yang Y 2020 *Thermal design of a hybrid cooling system for air-gap flux permanent magnet machines. IEEE Transactions on Magnetics* **56**(6) pp 1-9
- [11] Giulii Capponi F, De Donato G and Caricchi F 2012 *Recent advances in axial-flux permanent-magnet machine technology. IEEE Transactions on Industry Applications* **48**(6) pp 2190-2205
- [12] Vainel G, Staton D A, Giulii Capponi F, De Donato G and Caricchi F 2013 *Thermal modelling of a fractional-slot concentrated-winding kaman type axial-flux permanent-magnet machine. 2013 IEEE Energy Conversion Congress and Exposition* pp 1505-1511
- [13] Chai F, Bi Y and Chen L 2020 *A Comparison between Axial and Radial Flux Permanent Magnet In-Wheel Motors for Electric Vehicle. International Conference on Electrical Machines (ICEM)* pp 1685-1690
- [14] Gai Y, Kimiabeigi M, Chong Y C, Widmer J D, Deng X, Popescu M, Goss J, Staton D A and Steven A 2019 *Cooling of Automotive Traction Motors: Schemes, Examples, and Computation Methods. IEEE Transactions on Industrial Electronics* **66**(3) pp 1681-1692
- [15] Marcolini F, De Donato G and Caricchi F 2019 *Direct Oil cooling of End windings in Tour-Type Axial-Flux Permanent-Magnet Machines. IEEE Energy Conversion Congress and Exposition (ECCE)* pp 5645-5651
- [16] Dombek G and Nadolny Z 2018 *Influence of paper type and liquid insulation on heat transfer in transformers. IEEE Transactions on Dielectrics and Electrical Insulation* **25**(5) pp 1863-1870
- [17] Ning F, Wang Y, Yang L and Wang E 2020 *Research on Viscosity-Temperature Characteristics of PAO Oil and Ester Oil. Int. J. Of Eng. Res. & Tec. (IJERT)* **9**(6)
- [18] Edelsbrunner H 2009 *Geometry and topology for mesh generation*, Cambridge University press
- [19] Wang C, Qu R, Li J, Fan X, Li D and Lu Y 2017 *Rotor loss calculation and thermal analysis of a dual-stator axial-flux permanent magnet machine with combined rectangle-shaped magnets. 20th International Conference on Electrical Machines and Systems (ICEMS)* pp 5.